

# Dual-Programmable Shape-Morphing and Self-Healing Organohydrogels Through Orthogonal Supramolecular Heteronetworks

Ziguang Zhao, Shuyun Zhuo, Ruochen Fang, Longhao Zhang, Xintao Zhou, Yichao Xu, Jianqi Zhang, Zhichao Dong, Lei Jiang, and Mingjie Liu\*

Programmable materials that can change their inherent shapes or properties are highly desirable due to their promising applications. However, among various programmable shape-morphing materials, the single control route allows temporary states to recover the unchangeable former state, thus lacking the sophisticated programmability for their shape-encoding behaviors and mechanics. Herein, dual-programmable shape-morphing organohydrogels featuring supramolecular heteronetworks are developed. In the system, the metallo-supramolecular hydrogel framework and micro-organogels featuring semicrystalline comb-type networks independently respond to different stimuli, thereby providing orthogonal dual-switching mechanics and ultrahigh mechanical strength. The supramolecular heteronetworks also possess excellent self-healing properties. More notably, such orthogonal supramolecular heteronetworks demonstrate hierarchical shape morphing performance that far exceeds conventional shape-morphing materials. Utilizing this dual programming strategy of the orthogonal supramolecular heteronetworks, the material's permanent shape can be manipulated in a step-wise shape morphing process, thereby realizing sophisticated shape changes with a high degree of freedom. The organohydrogels can act as a biomimetic smart device for the on-demand control of unidirectional liquid transport. Based on these characteristics, it is anticipated that the supramolecular organohydrogels may serve as adaptive programmable materials for a variety of applications.

for applications in aerospace, smart devices, and biomedical materials.<sup>[1–3]</sup> Among these materials, shape-morphing polymers (SMPs) are particularly attractive because their forms can be programmed to perform transformations or motions in response to external stimuli (e.g., temperature, light, solvent, and electric fields).<sup>[3–11]</sup> Currently, two general approaches are used to obtain unparalleled shape-programming flexibility. The first involves geometric assistances to produce complex SMP shapes, such as kirigami and origami art, as well as 3D printing.<sup>[12–17]</sup> Alternatively, another approach is through the use of an innovational polymer network design, which employs functional components to expand the programmability of SMPs.<sup>[18–23]</sup> For example, SMPs with dynamic covalent polymer networks and reversible crosslinking netpoints exhibit unique shape reconfiguration and programmability.<sup>[18–21]</sup> However, despite these exciting prospects, most SMPs with the single control routes only allow complex temporary shapes to recover a former permanent state, ultimately limiting the versatility of these materials and our

ability to control them for complex applications. Owing to the intrinsic restriction of the permanently crosslinked polymer network, such single programming inevitably lacks a mechanism


ability to control them for complex applications. Owing to the intrinsic restriction of the permanently crosslinked polymer network, such single programming inevitably lacks a mechanism

Dr. Z. G. Zhao, Dr. S. Y. Zhuo, R. C. Fang, L. H. Zhang, X. T. Zhou, Y. C. Xu, Prof. L. Jiang, Prof. M. J. Liu  
Key Laboratory of Bio-Inspired Smart Interfacial Science and Technology of Ministry of Education  
School of Chemistry  
Beihang University  
Beijing 100191, P. R. China  
E-mail: liumj@buaa.edu.cn  
Prof. J. P. Zhang  
National Center for Nanoscience and Technology  
Beijing 100191, P. R. China

Prof. Z. C. Dong, Prof. L. Jiang  
Key Laboratory of Bio-inspired Smart Interface Sciences  
Technical Institute of Physics and Chemistry  
Chinese Academy of Sciences  
Beijing 100191, P. R. China

Prof. M. J. Liu  
International Research Institute for Multidisciplinary Science  
Beihang University  
Beijing 100191, P. R. China

Prof. M. J. Liu  
Beijing Advanced Innovation Center for Biomedical Engineering  
Beihang University  
Beijing 100191, P. R. China

 The ORCID identification number(s) for the author(s) of this article can be found under <https://doi.org/10.1002/adma.201804435>.

DOI: 10.1002/adma.201804435

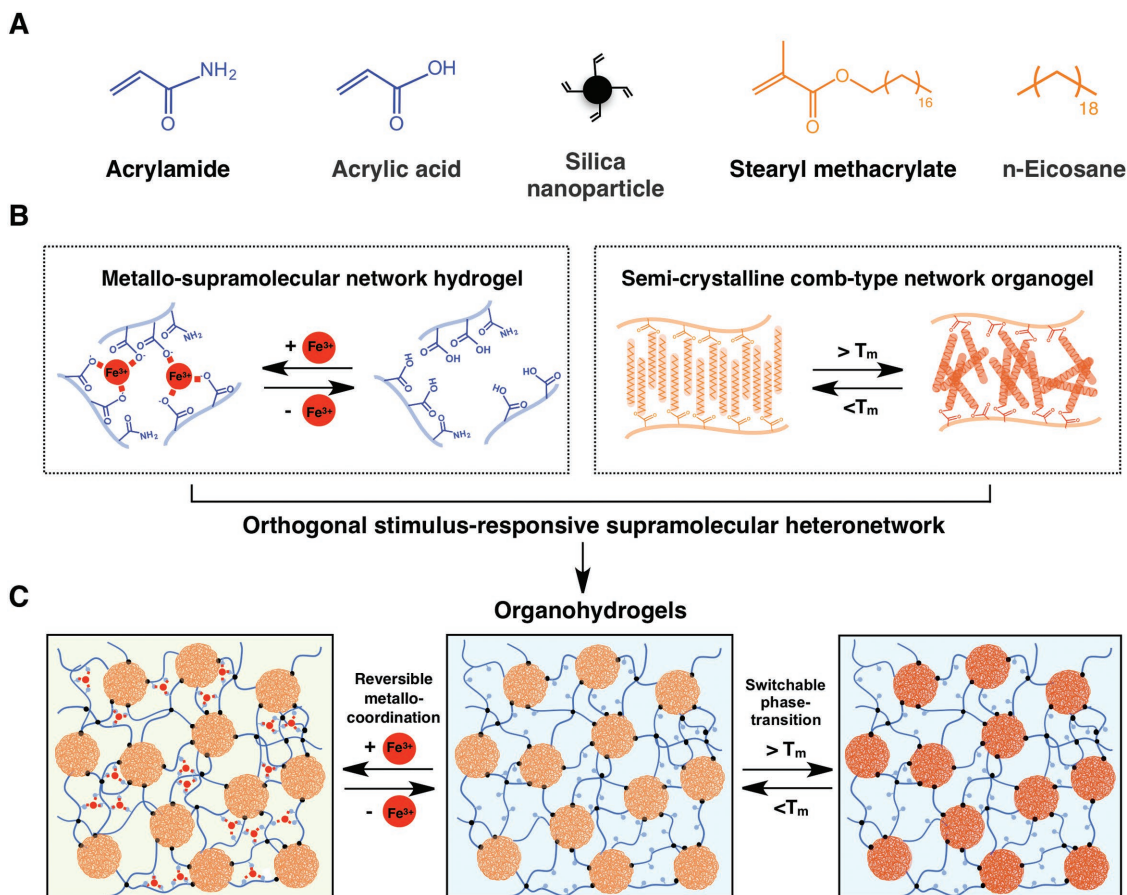


**Figure 1.** Schematic representation of the orthogonal dual-programmable mechanism of the supramolecular heteronetwork organohydrogel. A) Chemical structures of acrylamide, acrylic acid, oleophilic stearyl methacrylate, n-eicosane, and a schematic of the vinyl functionalized silica nanoparticles (VSNPs). B,C) Schematic illustration of the dual-phase heteronetwork structures and the orthogonal stimuli-responsive interactions of the supramolecular organohydrogels.

for further manipulating multistage shape evolution. Thus, the development of hierarchical programmable materials with a higher degree of freedom has remained a challenge.

Herein, we develop a dual-programmable shape-morphing organohydrogel that features spatially heterogeneous supramolecular networks (Figure 1). Due to the integration of micro-organogel inclusions featuring phase-transition comb-type networks with a reversible metallo-supramolecular hydrogel framework, our organohydrogels demonstrate both ultrahigh mechanical strength and orthogonal dual-switching mechanics. Additionally, our dynamic supramolecular heteronetworks provide a complementary effect to obtain excellent self-healing property. Importantly, utilizing this orthogonal dual-programmable strategy of the supramolecular heteronetworks, our materials possess hierarchical shape morphing behavior that enables versatile step-wise memorization and programming of geometrically complex structures. In this work, we demonstrate the manipulation of the material's permanent shape-encoding in hierarchical shape morphing process, thereby realizing sophisticated origami, kirigami, and multidimensional shape morphing evolution. Such unique programmable shape morphing performance is still extremely challenging to achieve in conventional SMPs. To demonstrate the applicability of our

materials, we show how these materials can act as a biomimetic smart device for controlling the unidirectional liquid transport. Due to these properties, our supramolecular organohydrogels would be ideal candidates for a variety of applications that are difficult to realize with conventional adaptive materials, including soft robots, biofluidic devices, and biomedical compounds.

In biological tissues, a myriad of distinct biomolecules such as proteins, DNA, and RNA spontaneously elicit orthogonally autonomic functionality, enabling the precise ability to control and regulate dynamic structures, metamorphoses, and the migration of live cells.<sup>[24–26]</sup> Inspired by such multicomponent natural systems, we hypothesized that a similar orthogonal and synergistic principle could be applied to the design of smart soft materials with sophisticated programming capabilities.

To achieve this aim, we employed an in situ heterophase emulsion polymerization technique to fabricate a dual-programmable shape-morphing, self-healable organohydrogel with a spatial supramolecular heteronetwork. The aqueous hydrogel precursor solution consisted of acrylamide and acrylic acid monomers, as well as vinyl functionalized silica nanoparticles (VSNPs) (Figure 1A). The VSNPs featured an average diameter of 10 nm, serving as a solid emulsifier due to their Pickering

effect, and used as nanocrosslinkers to maintain the hydrogel framework (Figure S1, Supporting Information).<sup>[27,28]</sup> The oil phase containing molten oleophilic stearyl methacrylate monomers and n-eicosane was emulsified in the aqueous phase to form a stable emulsion (Figure 1A; Figure S2, Supporting Information). After the gelation process, the resulting heterogeneous networks could be clearly visualized using confocal laser scanning microscopy (CLSM) and scanning electron microscopy (Figures S3 and S4, Supporting Information). We observed that the hydrogel framework continuously surrounded and individually isolated these micro-organogels, which featured diameters of 1–5  $\mu\text{m}$ . The micro-organogels were also uniformly distributed in the hydrogel framework, which was continuously linked due to the covalent interaction at the heterogeneous interface, resulting in a dual-phase organohydrogel network.

In the continuous hydrogel framework, we used tridentate Fe(III)–carboxylate coordination with the strong metal–ligand interactions to effectively reconfigure the network structures and improve the mechanical strength of organohydrogels (Figure 1B). The VSNPs within the hydrogel network act as stress buffers to homogenize the distribution of stress, with hydrogen bonds within the material also serving as reversible sacrificial bonds. The combination of strong and weak supramolecular interactions provides both high mechanical strength and energy dissipation mechanisms for the continuous hydrogel framework. Equally importantly is the dynamically controlled association/dissociation interaction of the metallo-supramolecular hydrogel network, which effectively switches the mechanical performance of the organohydrogel. Meanwhile, during emulsion polymerization, the oleophilic stearyl methacrylate monomers with long alkyl chains can form a semicrystalline comb-type network featuring a melting-crystallization transition. Additionally, n-eicosane as the dispersed phase has the same melting ( $T_m$ ) and crystallization ( $T_{\text{cryst}}$ ) temperature as the poly (stearyl methacrylate) network. These micro-organogel inclusions with switchable phase-transition property can further control the heteronetwork properties (Figure 1B). Based on such two-distinct supramolecular interactions derived from the dual-phase heteronetworks, our organohydrogels demonstrate orthogonally responsive properties by the manipulation of specific external stimuli (i.e., each homogenous network responds to an external stimulus that can be controlled independently) (Figure 1C).

Through the incorporation of the semicrystalline comb-type network micro-organogels into the metallo-supramolecular hydrogel framework, the material exhibited orthogonal dual-switching mechanics and ultrahigh mechanical strength. Hereafter, we will refer to our samples as organohydrogels<sub>x</sub> and organohydrogels<sub>x</sub>–Fe, in which  $x$  refers to the molar fraction of acrylic acid in the hydrophilic monomers and Fe refers to the samples with Fe(III) metal–ligand interactions. **Figure 2A** shows compressive strain–stress curves of the gel samples, demonstrating that the metallo-supramolecular hydrogel framework greatly enhances the mechanical strength of the organohydrogels. The enhanced mechanical strength of organohydrogels<sub>x</sub>–Fe has a strong dependence on the molar fraction of acrylic acid (Figure 2B; Figure S5, Supporting Information). When increasing the molar fraction of acrylic acid from 0.1 to 0.2, the compressive strength of the organohydrogels<sub>x</sub>–Fe increased from 10.9 to 32.8 MPa at 70% compressive strain

without any mechanical fracturing. By contrast, the corresponding organohydrogels without metal–ligand interactions displayed relatively weak mechanical strength (2.6–4.1 MPa). Note that the organohydrogels<sub>0.2</sub>–Fe yielded a high elastic modulus of 56.8 MPa at 10% strain, which was  $\approx 52$  times that of the organohydrogels<sub>0.2</sub>'s modulus and even 500 times greater than the original hydrogel framework. These results confirm that the strong metal–ligand association and rigid crystalline interaction of the dual-phase heteronetworks synergistically produce ultrahigh mechanical strength for a gel material.

The organohydrogels also exhibited the orthogonal metal-/thermoswitchable mechanics by manipulating specific external stimuli. The organohydrogels' elastic modulus and mechanical strength are obviously affected by the reversible metal–ligand association/dissociation of the hydrogel framework (Figure 2C). In the iterative process of the metal–ligand association/dissociation, the organohydrogels<sub>0.2</sub>–Fe maintained a high elastic modulus (52.9–57 MPa). To remove the Fe(III) ions bound in the hydrogel network, we transferred the sample into EDTA solution, and observed that the elastic modulus decreased to 0.97–1.2 MPa. This metal-tunable mechanical behavior is also observed in the materials' rheological properties. Figure S6 of the Supporting Information reveals a dynamic switch in the storage moduli ( $G'$ ) of our organohydrogels by manipulating the metallo-supramolecular interactions. Moreover, the  $T_m$  and  $T_{\text{cryst}}$  of the organohydrogels were measured to be 37.4 and 27.8  $^{\circ}\text{C}$ , respectively (Figure S7, Supporting Information). In Figure 2D, the samples' rheological measurements not only reflect the metal-enhanced mechanical properties, but also demonstrate its thermomechanical performance. The results further indicate that such thermoswitching behavior of the micro-organogels is not affected by the metal–ligand association of the hydrogel framework, thus acting as another independent mechanical switching mode. Figure 2E shows that  $G'$  of organohydrogels<sub>0.2</sub>–Fe decreases with increased temperature. During the phase-transition circulating process, the dynamic stability of the thermoswitchable mechanics of the organohydrogels<sub>0.2</sub>–Fe samples is fully demonstrated (Figure 2F). In the compressive test, the organohydrogels<sub>0.2</sub>–Fe sample yielded a low elastic modulus of 2.4 MPa at 10% strain and 60  $^{\circ}\text{C}$  ( $T > T_m$ ), which is  $\approx 4\%$  of the modulus at 20  $^{\circ}\text{C}$  ( $T < T_m$ ) (Figure S8, Supporting Information). Meanwhile, organohydrogels<sub>0.2</sub> featured a tensile fracture stress of 0.54 MPa and a fracture strain of 330% at 20  $^{\circ}\text{C}$  (Figure 2G). However, when heating the material above the  $T_m$ , the fracture stress decreased to 0.055 MPa and the fracture strain increased to  $\approx 1400\%$ . In this case, when  $T > T_m$ , the micro-organogel network with its noncrystalline alkyl side chains and molten dispersed phase becomes flexible and elastic, thereby enhancing the high-strain capacity of organohydrogels.

These dual-phase heteronetworks also provide a complementary supramolecular interaction for the realization of excellent self-healing behavior. The continuous hydrogel framework possesses a self-healing capacity that arises from the dynamic and reversible noncovalent interactions of the polymer network, including abundant hydrogen bonds and physical entanglements. Additionally, the micro-organogel inclusions with strong hydrophobic associations and a melting-crystalline transition further elicits the material's self-healing behavior. To confirm this property, we cut a virgin organohydrogel sample into

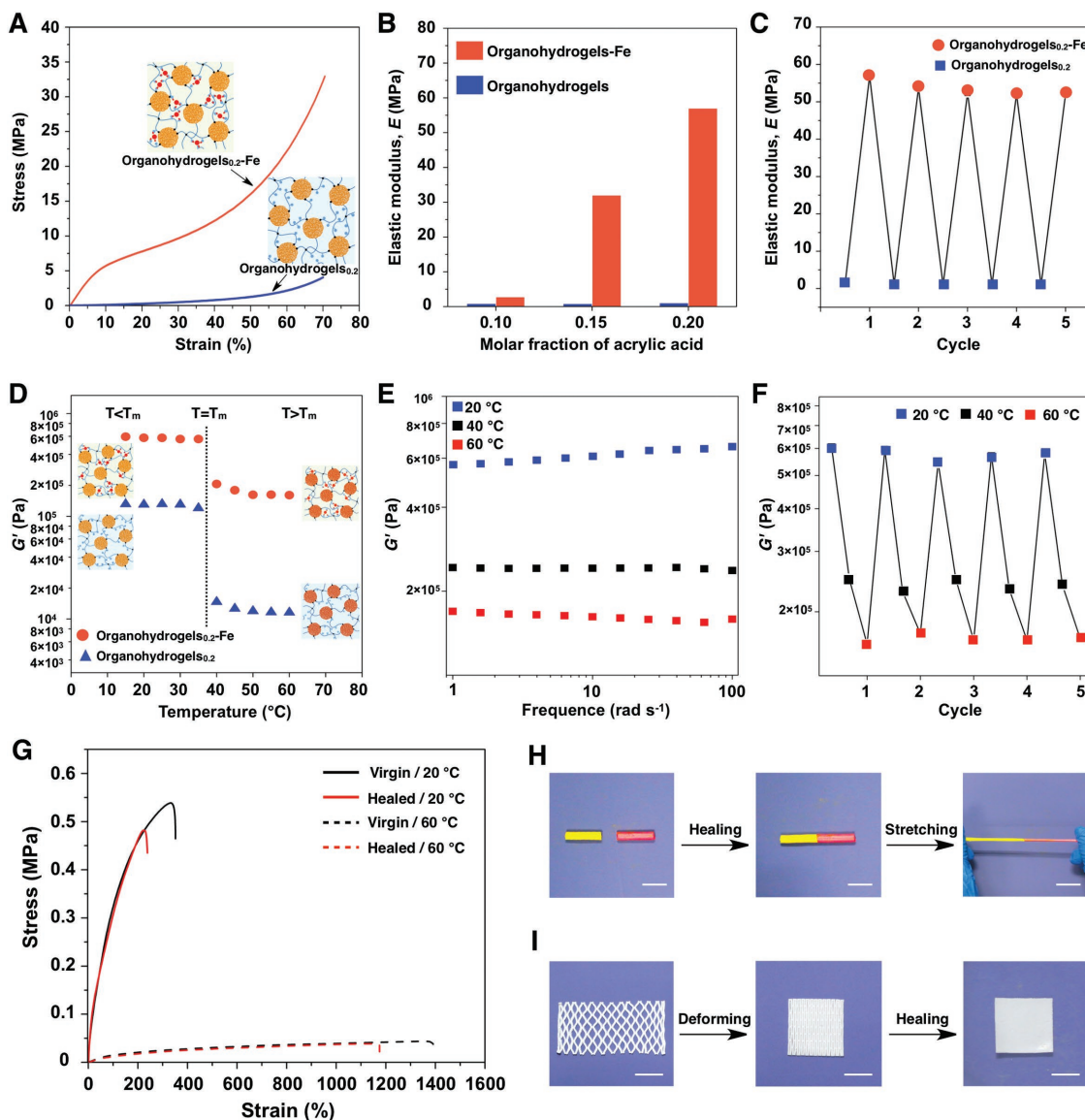


**Figure 2.** Orthogonal metallo-/thermoswitching mechanics and self-healing behavior of the organohydrogels. A) Compressive strain–stress curves of organohydrogels<sub>0.2</sub> and organohydrogels<sub>0.2</sub>-Fe. B) The tangent elastic moduli of the organohydrogels with different molar fractions of acrylic acid at 10% strain. C) Metal-tunable mechanics of organohydrogels<sub>0.2</sub> during the reversible metal–ligand association/dissociation process. D,E) The storage moduli ( $G'$ ) of organohydrogels<sub>0.2</sub>-Fe at a frequency ( $\omega$ ) sweep of 15.8 rad s<sup>-1</sup> and varied temperatures exhibits thermoswitchable mechanics. F) The stable thermoswitchable mechanics of organohydrogels<sub>0.2</sub>-Fe in the phase-transition crystallization/melting circulating process of the micro-organogel inclusions. G) Tensile strain–stress curves of virgin and healed organohydrogels<sub>0.2</sub>. H) Images showing how the healed organohydrogels<sub>0.2</sub> easily withstand stretching at a temperature above the melting temperature ( $T_m$ ) of the micro-organogel inclusions. I) Images of the self-healing effect of the organohydrogels<sub>0.2</sub>, featuring kirigami-based structures.

two halves, and subsequently reattached them together. After 1 h heating ( $T = 60^\circ\text{C}$ ), the separated pieces adhered again to obtain one gel. The healed samples could again sustain large strain deformation at  $T > T_m$  (Figure 2H). We can extend this self-healable capacity to repair the high-density and complex cuts. We prepared an organohydrogel film with kirigami-based structure containing abundant patterned incisions (Figure 2I). During the simple heating process, all the cuts were readily healed to obtain the complete film. The tensile stress–strain measurements show that the healed organohydrogel features high mechanical performance and has a high-strain capacity

(Figure 2G). Combining ultrahigh mechanical strength, orthogonal binary switching mechanics, and self-healing properties, we anticipate that these organohydrogels would be ideal candidates for bioengineering applications that are difficult to achieve using conventional adaptive gel materials.

Based on the synergistic and orthogonal supramolecular interactions of the dual-phase heteronetworks, the organohydrogels exhibit unique hierarchical shape morphing behavior. The conventional SMPs can “memorize” one-single permanent shape because of nondynamic permanent polymer networks. Thus, the general programming principle of these materials is

based on a single control route that allows for programming complex temporary shapes that can only recover unchangeable original state. By contrast, our hierarchical shape morphing effect emphasizes the multistage shape morphing evolution that enables versatile step-wise memorization and programming of geometrically complex shapes through the orthogonal dual-programmable strategy. The specific permanent shapes can be memorized and erased at different hierarchy levels of shape morphing process, similar to a flash drive that can be reprogrammed and reformatted, thereby expanding materials' versatile and sophisticated shape morphing performance.

**Figure 3A** illustrates the dual-programmable mechanism for hierarchical shape morphing performance, in which the permanent shape memorization process is referred to as Route A, and

the shape memory process as Route B. In the case of Route A, the metallo-supramolecular hydrogel framework dominates the permanent shape memorization process via the strong metal–ligand interactions. Route B mainly originates from the thermoswitchable phase-transition of the micro-organogel inclusions. The incorporation of the controllable elasticity effect and the interfacial tension of the heteronetworks effectively manipulates the shape fixing and recovery during Route B. In the original shape state, organohydrogels maintain the lowest energy. When temperature is set above  $T_m$ , the soft micro-inclusions result in the easy processing of gel samples. At  $T < T_m$ , the crystalline interactions of the micro-organogels fix their deformed shape, restricting shape recovery of the elastic hydrogel framework by the covalent interconnections within

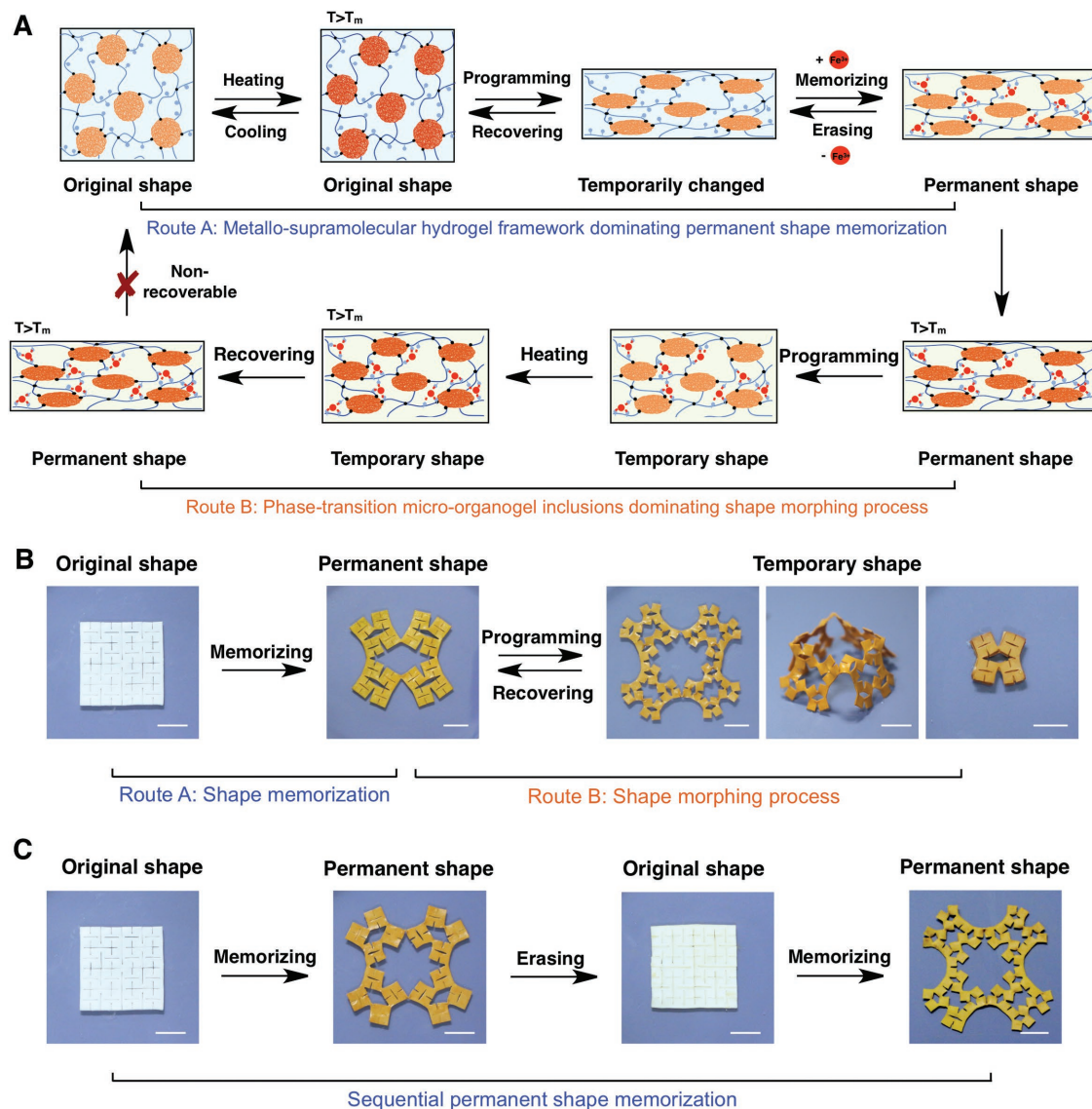


**Figure 3.** Hierarchical shape morphing performance of the supramolecular heteronetwork organohydrogels. A) Illustration of the dual-programmable shape morphing behavior. The top row shows the gel's permanent shape memorization process, which is dominated by the reversible metallo-supramolecular hydrogel framework (Route A). The bottom row shows that phase-transition micro-organogel inclusions dominate the shape morphing process of the organohydrogels (Route B). B) Images show the hierarchical shape morphing performance of the organohydrogels into complex kirigami-based structures. C) Images indicate the sequential permanent kirigami shape memorization. The scale bar is 1 cm.

the heteronetworks. During activation of the metal–ligand interactions in Route A, the topological network reconfiguration can depress the storage energy of the previous temporary state and form a permanently charged heteronetwork structure, even at high temperature ( $T > T_m$ ). Note that in our case, any permanent shape can be reversibly erased and memorized via the associative/dissociative interactions of the metallo-supramolecular hydrogel framework. Compared with reported SMPs featuring dynamic covalent networks, our permanent shape memorization process does not rely on added external stress or catalysis, making it simple and reliable.<sup>[19,20]</sup>

The integration of permanent shape memorization and shape morphing behavior offers the unique opportunity to program sophisticated shape evolution that is far beyond the conventional shape morphing scope. In particular, we utilized kirigami and origami techniques to illustrate such highly complex shape morphing effects. For example, our original shape was a square film featuring smaller square-patterned kirigami structures. These square pattern units within the flat film can be deformed or fixed by shape memory process (Figure S9, Supporting Information). The step-wise deformations of these complex kirigami-based structures are shown

in the schematic of Figure S10 of the Supporting Information. Through activating route A, this original square film was programmed into an expanded permanent shape. In the next shape morphing evolution hierarchy, this expanded permanent shape can be programmed into various recoverable temporary shapes, including a highly expanded film, a 3D braced structure, and a multifolded shape using shape memory effect (Figure 3B). Note that the permanent shape can also be sequentially memorized and erased in the hierarchical shape morphing process (Figure 3C). During Route A, we observed that the white samples turned yellow in color, indicating the formation of metal–ligand bonds as the supramolecular configured units into the permanent shape state. Similarly, with extensive folding deformation, a 2D rhombic film can be used to create a 3D origami shape of a swan (Figure 4A). In Figure S11 of the Supporting Information, we demonstrate how to fold the related 3D origami shapes. Meanwhile, we manipulated the opposite shape morphing in the next stage. In our case, this origami permanent shape can be programmed into the recoverable temporary film. Through a step-wise memorization process, various complex permanent origami shapes can be sequentially obtained (Figure 4B).

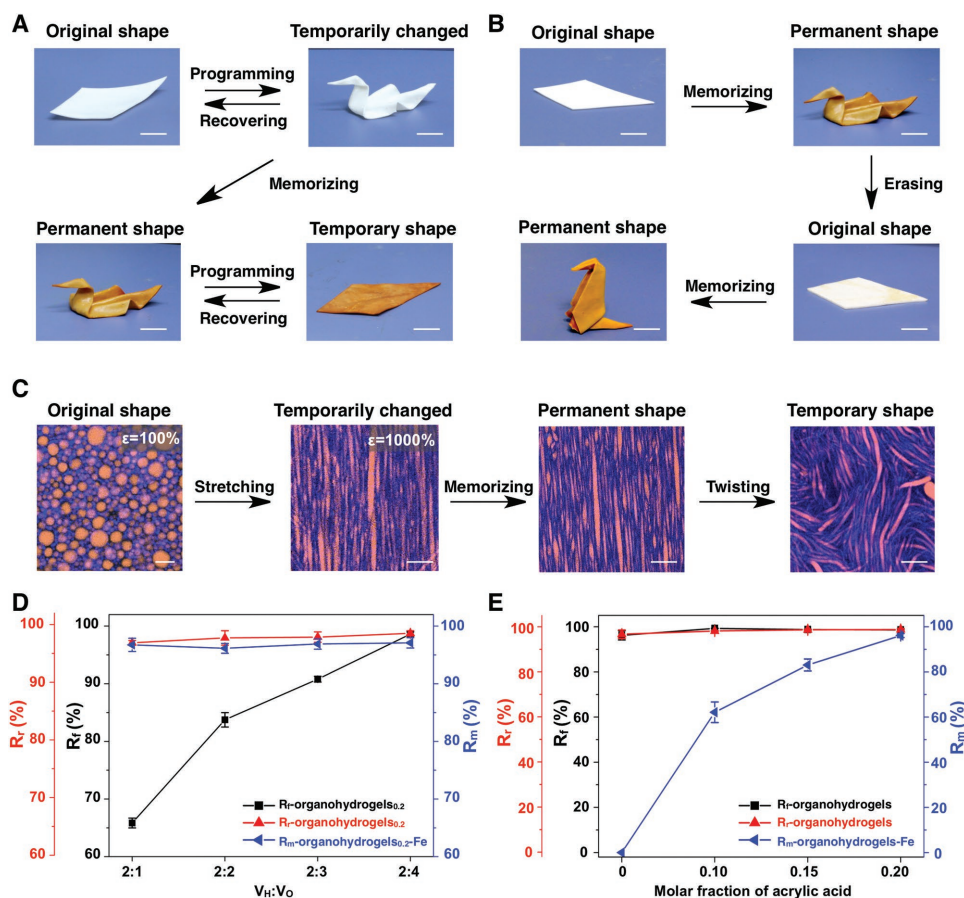


**Figure 4.** Hierarchical shape morphing process and quantitative characterization. A,B) Images showing the origami shape changes and sequentially configured permanent origami shapes of the organohydrogels. The scale bar is 1 cm. C) CLSM images show the real-time observation of the internal heteronetwork structures of the organohydrogel during the hierarchical shape morphing process. The scale bar is 5  $\mu\text{m}$ . D) The shape fixity ratio ( $R_f$ ), the shape recovery ratio ( $R_r$ ), and the shape memorization ratio ( $R_m$ ) of the organohydrogels with different volume ratios of the hydrogel ( $V_H$ ) and micro-organogel ( $V_O$ ) components. E)  $R_f$ ,  $R_r$ , and  $R_m$  of the organohydrogels with different molar fractions of acrylic acid.

Equally importantly, during the dual-programmable process, our supramolecular organohydrogels achieve the high-strain and stiffness shape morphing effect (Figure S12, Supporting Information). Currently, the importance of dynamically controllable mechanics of SMPs can be easily overlooked. Conventional SMPs generally lack extra mechanical control mechanisms for adapting complex shape manipulation. In our case, the original organohydrogels exhibit fully recoverable strains of up to 1000% through thermal stimuli, thus can be identified as high-strain shape morphing materials by comparison with the deformability of the previously reported SMPs.<sup>[7]</sup> Such a highly strained shape can be further memorized to form a stable permanent structure due to the topological network reconfiguration derived from the metallo-supramolecular hydrogel framework. As such, the metal-enhanced mechanical strength of organohydrogels–Fe elicits the high stiffness property, which can provide adequate support for a specific temporary shape state.

During this high-strain shape morphing process, the heteronetwork morphology of organohydrogels was verified by CLSM and small-angle X-ray scattering (SAXS). In Figure 4C and Figure S13 (Supporting Information), we observed the shape programming process of the micro-organogels change from an isotropic spherical shape to an aligned ellipsoidal permanent shape, and then to a twisting temporary shape. From the

corresponding anisotropic to isotropic scattering patterns, we confirmed that such a highly strained alignment structure can be memorized, and further erased to the isotropic structure (Figure S14, Supporting Information). We also investigated the shape fixity ratio ( $R_f$ ), the shape recovery ratio ( $R_r$ ), and the shape memorization ratio ( $R_m$ ) of organohydrogels<sub>0.2</sub> with different volume ratios of the hydrogel ( $V_H$ ) and micro-organogel ( $V_O$ ) components (Figure 4D,E).  $R_f$  decreased with decreasing micro-organogels, which suggests that the low-ratio fixed micro-organogels cannot restrict the recovery effect of the hydrogel network. The  $R_m$  of the organohydrogels<sub>0.2</sub> with different  $V_H$  and  $V_O$  approaches 100%, because enough metallo-supramolecular units of the organohydrogels<sub>0.2</sub> can maintain a stable permanent shape. By contrast, with decreasing molar fraction of acrylic acid,  $R_m$  of the organohydrogels with fixed hydrogel and micro-organogel components ( $V_H:V_O = 1:2$ ) decreased due to the diminished number of metallo-supramolecular configured units, leading to an insufficient topological network reconfiguration.

In addition to sophisticated hierarchical kirigami and origami shape changes, our supramolecular organohydrogels also realize step-wise multidimensional shape morphing behaviors which can provide additional degrees of freedom for shape manipulation from 2D microstructures to 3D geometric designs (Figure 5A,B; Figure S15, Supporting Information).

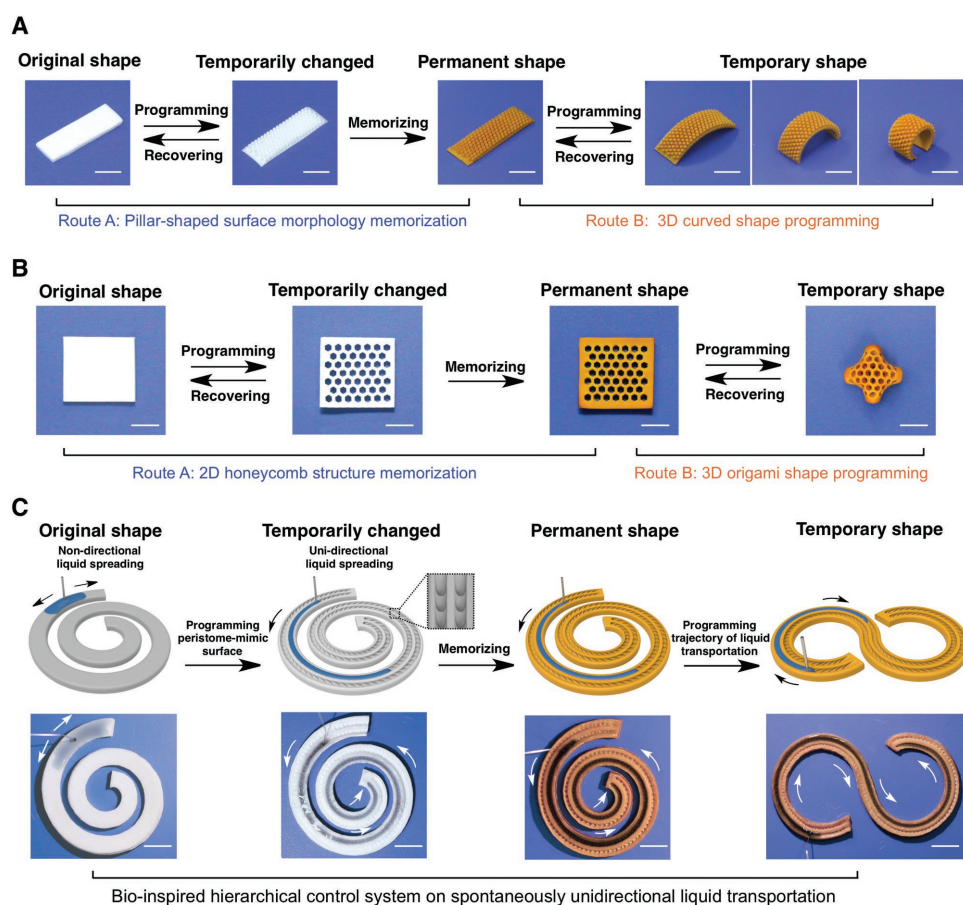


**Figure 5.** Step-wise multidimensional shape changes. A,B) The step-wise shape changing process from a permanent 2D morphology memorization to a recoverable temporary 3D shape programming. C) Spontaneous unidirectional liquid transport manipulated during the step-wise multidimensional shape changing process. The images show dyed ethanol moving in one direction on a peristome-mimetic organohydrogel surface. The scale bar is 1 cm.

In this study, we programmed the organohydrogel film surface to obtain microstructures, such as pillar-shaped and honeycomb morphologies. We activated route A to permanently memorize these 2D microstructure. In the next shape morphing stage, we further manipulated the 3D shape memory capability of our material with the permanent 2D morphologies (Movie S1, Supporting Information). Such step-wise multidimensional shape change is nearly impossible to achieve with conventional SMPs. Thus, these supramolecular organohydrogels may provide promising utility for smart devices to suit a variety of applications.

Inspired by the liquid transport derived from the peristome surface of *Nepenthes alata*,<sup>[29,30]</sup> a carnivorous pitcher plant that uses surface wetting changes to capture prey, we programmed a peristome-mimicking organohydrogel surface to realize spontaneously unidirectional liquid spreading (Figure 5C). We note that dyed ethanol can spontaneously spread on a spiral surface in a unidirectional fashion. Through step-wise shape morphing manipulation from a spiral to serpentine shape, the trajectory of the liquid transportation can be accumulatively controlled (Movie S2, Supporting Information). This result demonstrates how our hierarchical shape morphing organohydrogels can act as ideal programmable materials for the on-demand manipulation of liquid in unidirectional transport, which has wide applications in biofluidic devices, nonpowered drug delivery, and self-lubrication engineering.

In conclusion, we developed a dual-programmable shape-morphing organohydrogel using an orthogonal supramolecular heteronetworks. The incorporation of a semicrystalline comb-type network of micro-organogels into the reversible metal-supramolecular hydrogel framework enables materials' ultrahigh mechanical strength and orthogonal dual-switching mechanics. Meanwhile, our heteronetworks provide a complementary effect to obtain excellent self-healing property. Owing to the unique dual-programmability of the orthogonal supramolecular heteronetworks, our organohydrogels demonstrate desirable hierarchical shape morphing capabilities that enable the step-wise manipulation of sophisticated origami, kirigami and multidimensional shape changes, far exceeding the conventional shape morphing capacity. Based on such behavior, these supramolecular organohydrogels can act as biomimetic smart device for the on-demand control of spontaneously unidirectional liquid transportation. Therefore, this organohydrogel design provides an ideal opportunity for the expanded application of programmable shape-morphing materials in areas such as soft robotics, smart devices, and bioengineering materials.

## Supporting Information

Supporting Information is available from the Wiley Online Library or from the author.

## Acknowledgements

Z.G.Z. and S.Y.Z. contributed equally to this work. This work was financially supported by the National Natural Science Funds for Distinguished Young Scholar (No. 21725401), the National Natural

Science Foundation of China (No. 21574004), the National Key R&D Program of China (No. 2017YFA0207800), the Fundamental Research Funds for the Central Universities, the National 'Young Thousand Talents Program', and the Academic Excellence Foundation of BUAA for PHD Students.

## Conflict of Interest

The authors declare no conflict of interest.

## Keywords

dual-programmable shape morphing, gel materials, orthogonal supramolecular heteronetworks, programmable materials, self-healing

Received: July 11, 2018

Revised: September 10, 2018

Published online:

- [1] J. A. Faber, A. F. Arrieta, A. R. Studart, *Science* **2018**, 359, 1386.
- [2] M. Montgomery, S. Ahadian, L. D. Huyer, M. L. Rito, R. A. Civitarese, R. D. Vanderlaan, J. Wu, L. A. Reis, A. Momen, S. Akbari, A. Pahnke, R. K. Li, C. A. Caldarone, M. Radisic, *Nat. Mater.* **2017**, 16, 1038.
- [3] F. Chen, D. Zhou, J. Wang, T. Li, X. Zhou, T. Gan, S. H. Wang, X. Zhou, *Angew. Chem., Int. Ed.* **2018**, 57, 6568.
- [4] R. M. Erb, J. S. Sander, R. Grisch, A. R. Studart, *Nat. Commun.* **2013**, 4, 1712.
- [5] X. Hu, J. Zhou, M. V. Varnosfaderani, W. F.M. Daniel, Q. Li, A. P. Zhushma, A. V. Dobrynin, S. S. Sheiko, *Nat. Commun.* **2016**, 7, 12919.
- [6] F. Ge, X. Lu, J. Xiang, X. Tong, Y. Zhao, *Angew. Chem., Int. Ed.* **2017**, 56, 6126.
- [7] Z. Zhao, K. Zhang, Y. Liu, J. Zhou, M. Liu, *Adv. Mater.* **2017**, 29, 1701695.
- [8] Z. Zhao, Y. Liu, K. Zhang, S. Zhuo, R. Fang, J. Zhang, L. Jiang, M. Liu, *Angew. Chem., Int. Ed.* **2017**, 56, 13464.
- [9] Z. Zhao, Y. Xu, R. Fang, M. Liu, *Chin. J. Polym. Sci.* **2018**, 36, 683.
- [10] L. Zhang, P. Naumov, X. Du, Z. Hu, J. Wang, *Adv. Mater.* **2017**, 29, 1702231.
- [11] Y. Yang, Z. Pei, Z. Li, Y. Wei, Y. Ji, *J. Am. Chem. Soc.* **2016**, 138, 2118.
- [12] T. C. Shyu, P. F. Damasceno, P. M. Dodd, A. Lamoureux, L. Xu, M. Shlian, M. Shtein, S. C. Glotzer, N. A. Kotov, *Nat. Mater.* **2015**, 14, 785.
- [13] L. Xu, T. C. Shyu, N. A. Kotov, *ACS Nano* **2017**, 11, 7587.
- [14] A. Kotikian, R. L. Truby, J. W. Boley, T. J. White, J. A. Lewis, *Adv. Mater.* **2018**, 30, 1706164.
- [15] A. S. Gladman, E. A. Matsumoto, R. G. Nuzzo, L. Mahadevan, J. A. Lewis, *Nat. Mater.* **2016**, 15, 413.
- [16] Z. Ding, C. Yuan, X. Peng, T. Wang, H. J. Qi, M. L. Dunn, *Sci. Adv.* **2017**, 3, e1602890.
- [17] L. Huang, R. Jiang, J. Wu, J. Song, H. Bai, B. Li, Q. Zhao, T. Xie, *Adv. Mater.* **2017**, 29, 1605390.
- [18] R. R. Kohlmeier, P. R. Buskohl, J. R. Deneault, M. F. Durstock, R. A. Vaia, J. Chen, *Adv. Mater.* **2014**, 26, 8114.
- [19] A. Oyefusi, J. Chen, *Angew. Chem., Int. Ed.* **2017**, 56, 8250.
- [20] Q. Zhao, W. Zou, Y. Luo, T. Xie, *Sci. Adv.* **2016**, 2, e1501297.
- [21] N. Zheng, Z. Fang, W. Zou, Q. Zhao, T. Xie, *Angew. Chem., Int. Ed.* **2016**, 55, 11421.
- [22] K. M. Herbert, S. Schrettl, S. J. Rowan, C. Weder, *Macromolecules* **2017**, 50, 8845.

- [23] T. Li, J. Wang, L. Zhang, J. Yang, M. Yang, D. Zhu, X. Zhou, S. H. Wang, Y. Liu, X. Zhou, *J. Mater. Chem. B* **2017**, 5, 5726.
- [24] B. Alberts, J. Wilson, T. Hunt, *Molecular Biology of the Cell*, 5th ed., Garland Science, New York **2008**, pp. 965–1052.
- [25] D. A. D. Parry, J. M. Squire, *Fibrous Proteins: Structures and Mechanisms*, Springer, Berlin **2017**.
- [26] H. Shigemitsu, T. Fujisaku, W. Tanaka, R. Kubota, S. Minami, K. Urayama, I. Hamachi, *Nat. Nanotechnol.* **2018**, 13, 165.
- [27] W. P. Hohenstein, H. Mark, *J. Polym. Sci.* **1946**, 1, 549.
- [28] Y. Huang, M. Zhong, F. Shi, X. Liu, Z. Tang, Y. Wang, Y. Huang, H. Hou, X. Xie, C. Zhi, *Angew. Chem., Int. Ed.* **2017**, 56, 9141.
- [29] H. Chen, P. Zhang, L. Zhang, H. Liu, Y. Jiang, D. Zhang, Z. Han, L. Jiang, *Nature* **2016**, 532, 85.
- [30] C. Li, N. Li, X. Zhang, Z. Dong, H. Chen, L. Jiang, *Angew. Chem., Int. Ed.* **2016**, 55, 14988.